A quick earthquake disaster loss assessment method supported by dasymetric data for emergency response in China

Jinghai Xu[1], Jiwen An[2], Gaozong Nie[2,*]

[1]{College of Geomatics Engineering, Nanjing Tech University, Nanjing, China}

[2]{Institute of Geology, China Earthquake Administration, Beijing, China}

Correspondence to: G.Z. Nie (niegz@ies.ac.cn)

Abstract

Improving earthquake disaster loss estimation speed and accuracy is one of key factors in effective earthquake response and rescue. The presentation of exposure data by applying a dasymetric map approach has good potential for addressing this issue. With the support of 30" × 30" areal exposure data (population and building data in China), this paper presents a new two-phase earthquake disaster loss estimation method for emergency response situations. This method has two phases: a pre-earthquake phase and a co-earthquake phase. In the pre-earthquake phase, we pre-calculate the earthquake loss related to different seismic intensities and store them in a 30" × 30" grid format, which has four stages: determining the earthquake loss calculation factor, gridding damage probability matrices, calculating building damage and calculating people loss. The dasymetric map approach makes this possible. Then, in the co-earthquake phase, there are two stages of estimating loss: generating a theoretical isoseismal map to depict the spatial distribution of the seismic intensity field; then, using the seismic intensity field to extract statistics of disaster loss from pre-calculated loss estimation data. Thus, the final loss estimation results are obtained. The method is validated by four actual earthquakes that occurred in China. The method not only significantly improves the speed and accuracy of loss estimation, but also provides spatial distribution for the loss, which will be effective in aiding earthquake emergency response and rescue. Additionally, related pre-calculated earthquake loss estimation data in China could serve to provide disaster risk analysis before earthquakes happen. Currently, the pre-calculated loss estimation data and the two-phase estimation method are used by the China Earthquake Administration.

1 Introduction

Earthquakes are one of the most serious natural disasters in the world. For example, the 1994 Northridge earthquake in the U.S.A. caused $12.5 billion insurance losses (NRC, 1999); the Bam earthquake in Iran (2003) resulted in more than 30,000 deaths (Nadim et al., 2004); 69,227 people died and 17,923 people were lost in Wenchun earthquake in China (2008) (China Earthquake Administration, 2010). Unfortunately, accurate earthquake prediction is still a difficult and even impossible task. In such situations, post-earthquake emergency response and rescue services have been used in many real earthquake scenarios to mitigate the disaster in China. These have already proven their efficiency many times in earthquake disaster mitigation (Earthquake Emergency Rescue Department, 2004). Many real earthquake rescues have shown how prompt and correct decision-making about rescue countermeasures are crucial for success. Since more than 72 hours after an earthquake, the survival ratio of people buried in destroyed buildings sharply decreases, the period after the earthquake has been known as the "golden 72 hours" (Xu et al., 2013). Generally, after a destructive earthquake, it is necessary to bring in rescue teams from outside the disaster area, and it will take much time (generally more than two days) for them to gather, to be dispatched and to move in, especially in mountainous areas.

Quick and effective rescue decision-making is based on the understanding the disaster information, even if it is not very accurate disaster information. However, there is a "black-box effect" of co-earthquake and post-earthquake disaster information, which means it is almost impossible to obtain useful disaster information within the first 1 to 2 hours after an earthquake (Nie et al., 2012). As an alternative, descriptive earthquake parameters (i.e. earthquake magnitude, peak ground acceleration – PGA) have been used as inputs to estimate the possible losses and to provide emergency disaster information, in which possible building damage and loss of life are the most important information.

China is a country that suffers from serious earthquake disasters. Due to its large land territory and high population, the Chinese government has very high real-time requirements for co-earthquake disaster loss estimation (especially people loss). Generally, it takes only 30 minutes for experts from the China Earthquake Administration (CEA) to estimate the disaster loss and to prepare suggestions on the rescue countermeasures (Miao et al., 2004). Even for a huge earthquake like the Wenchuan earthquake (Ms 8.0), the first earthquake loss estimation

and rescue countermeasures have to be submitted to the central government within one hour of the earthquake. However, performing the current earthquake disaster loss estimation methods used by the CEA needs more than twenty minutes, not including the time for the rescue countermeasure suggestions and other unexpected actions. Moreover, sometimes the accuracy of the estimation results even cannot correct to an order of magnitude compared to real disaster information. This has even delayed and misled the rescue decision-making in the response to China's Wenchuan earthquake. As the one of most serious disaster areas, Qinchuan County did not get an appropriate rescue response, while most of rescue materials were sent to less damaged Dujiangyan City. One of the reasons for this problem is that the disaster exposure data (population, buildings) are based on administrative units (census tracts).

A dasymetric map approach considers the spatial disparity of disaster exposure data and can improve the disaster estimation accuracy (Chen, 2004). With the support of our former project, a dasymetric exposure dataset (including population, building) has been developed. This study is focused on using these dasymetric data to improve the speed and accuracy of co-earthquake disaster loss estimation (building damage and people loss). This research work is part of the National Key Technology R&D Programme of China entitled, "Earthquake Disaster Information Service and Emergency Decision-making Support Platform". The project aims to develop rapid disaster information estimation and collection methods, and to dynamically generate emergency countermeasures for all levels of government.

The remainder of this paper is organized as follows: Section 2 presents research related to the study; Section 3 introduces the areal exposure data that will be used in this study, including population and building data covering the whole of China; Section 4 presents a two-phase earthquake disaster loss estimation method based on areal exposure data, consisting of the pre-earthquake phase and co-earthquake phase; Section 5 uses four real earthquake cases to validate the speed and accuracy of loss estimation with this estimation method, and discusses the results; and, Section 6 sets out the conclusions of this study.

2 Related research

Earthquake disaster loss estimation and risk analysis are key components of disaster management. From an approach fitted to the spatial range, the earthquake damage estimation model can be classified into a globally used model and locally used model. The globally used

model tries to estimate the earthquake disasters occurring over the world. A Prompt Assessment of Global Earthquakes for Response (PAGER) system has been developed by the US Geological Survey (USGS) to rapidly estimate possible the deaths and economic losses from an earthquake (http://earthquake.usgs.gov/earthquakes/pager/). This system can report economic losses and the affected people and the risk level within 30 minutes of a significant earthquake (magnitude more than 5.5). However, because of the spatial variability of the ground motion, the estimated disaster loss accuracy is reduced by inaccurate information on the shaking caused by the quake (Karimzadeh et al., 2014). Similar global (regional) systems include the Global Disaster Alert and Coordination System (GDACS; http://www.gdacs.org) and the World Agency of Planetary Monitoring and Earthquake Risk Reduction (WAPMERR; http://www.wapmerr.org). While the Global Earthquake Model (GEM; http://www.globalquakemodel.org) aims to provide software and tools for seismic risk assessment and loss estimation through a worldwide public-private partnership.

Generally, because earthquake loss estimation is a complex issue, different methods and parameters are needed for different areas of the world (Karimzadeh et al., 2014). Several local earthquake loss methods have been developed. Hazards United States Multi-Hazard (HAZUS-MH) is a well-known system (model) developed by Federal Emergency Management Agency (FEMA) in the USA. It can be used for multiple categories of natural disasters, including earthquakes. HAZUS-MH uses a building fragility curve to estimate possible damage, which is supported by census tract data. However, it is a time-consuming system. The preparation of rapid loss estimates for large study regions of 1000–2000 census tracts might require 0.5 to 1.5 hours of analysis time (FEMA, 2003). The Karmania hazard model is another GIS-based local earthquake disaster loss estimation method developed in Iran (Hassanzadeh et al., 2013).

Concerning the disaster estimation methods, many studies have focused on building damage estimation. However, people loss information is more important for earthquake emergency responses. Different levels of people loss mean different response and rescue levels, according to the *Chinese Earthquake Emergency Response Plan* (http://www.gov.cn/yjgl/2012-09/21/content_2230337.htm). However, actual earthquake disaster loss investigations during twentieth century have revealed that 75% of deaths come from building damage (Coburn and Spence, 2002). So generally, people losses are estimated by regression on building damage estimates. With regard to building damage estimation, two

kinds of method are widely used: the damage probability matrices (DPM) method and the fragility curve method. Whitman et al. (1973) first suggested the use of DPM to describe the building damage probability in earthquakes. It was firstly adopted by the Applied Technology Council (ATC-13) in 1985 (ATC, 1985). This method firstly classifies buildings into 36 types and this was later reduced to six types in ATC-21 (Mocormack, 1997). In this method, the building damage was classified into five categories: no damage, slight damage, moderate damage, serious damage and collapse. The building damage ratio for different damage degrees (e.g. slight damage, moderate damage) under different seismic intensities are presented as a matrix of the area struck by an earthquake. The fragility curve method is actually the transformed DPM, which use a fragility curve to represent the possible damage related to ground movement parameters.

There are three ways to obtain an appropriate DPM or building fragility curve: an empirical approach, an analytic approach and a hybrid approach. The empirical approach is based on statistics of real earthquake building damages and the setting up of a relationship between earthquake parameters (i.e. PGA, seismic intensity) and the degree of building damages (Anagnos et al., 1995). In the analytic approach, the DPM (or the building fragility curve) is derived from the mechanical analytic calculation for different types of building (Dymiotis et al., 1999). The hybrid approach simultaneously uses seismic hazard investigation data and building structure simulation analysis data to generate the DPM (or building fragility curve; Kappos et al., 2006).

Nowadays, the application of GIS is a growing trend and even a requirement for building damage estimation. GIS is widely used to manage and analyse disaster exposure data (Mebarki et al., 2014; Panahi et al., 2014; Armenakis, 2013; Alam et al., 2013). Organization of the exposure data in GIS has significantly influence on loss estimation speed and accuracy. Chen et al. (2004) and Thieken et al. (2006) elaborated the possible improvement in disaster loss analysis that can be obtained by the application of a dasymetric mapping approach in theory (more explanations in this paper are provided in the Figure 7). As one of measures of exposure, there are many discussions about areal population production. Jia et al. (2014) used the dasymetric approach to disaggregate population census data into a quadrilateral grid composed of 30 m $\times$ 30 m cells covering Alachua County, Florida. Alahmadi et al. (2013) produced a downscale population distribution of Riyadh, Saudi Arabia using remote sensing data and ward-level census population data. According to Thieken et al. (2006), there are four

categories of method for generating population dasymetric map using land cover data: the binary method, the three-class method, the limiting variable method and regression method.

In addition to the dasymetric map generation modelling studies, there are already some well-known areal data sets of the world's population, such as the Gridded Population of the World (GPW; Balk and Yetman, 2004), the Global Rural Urban Mapping Project (GRUMP; CIESIN, 2004), the LandScan Global Popultaion Databases (Dobson et al., 2000) and the WorldPop project (http://www.worldpop.org.uk/). The data scale generally ranges from 30" cells (longitude and latitude is 30", which is about 1 km at the equator) to 7.5" cells (about 250 m). In general, studies have focused on the algorithms for generating the dasymetric maps and the improving of the data spatial scale (Langford, 2007; Martin, 2011; Lin, 2011; Dmowska and Stepinski, 2014). Most studies have acknowledged the promising potential for applying these maps in disaster risk analysis and mitigation (Chakraborty et al., 2005).

By integrating the above studies and using areal exposure data, we will explore an earthquake disaster loss assessment method for application in Chinese mainland earthquake emergency response, with the aim of improving the speed and accuracy of estimation.

3 The input data

3.1 Dataset

Earthquake disaster exposure data are the foundation of disaster loss estimation. From the perspective of an earthquake emergency in China, these data have been named "earthquake emergency foundation data", which refers to the comprehensive data for earthquake disaster response and rescue, including a wide range of social, economic, population, city map, natural geographic landforms, key object location, rescue team information, relief communication and earthquake preplanning data (Nie et al., 2002). Over the last ten years, much progress has been made in the construction of earthquake emergency foundation data. Currently, each Chinese province built an earthquake emergency foundation database. Earthquake emergency foundation data gridding is the developing trend, disaggregating from administration units to areal grids, with the most popular representation of the data being the 30" × 30" cell size (about 1 km at the equator, which we abbreviate it as km grid).

With the support of project “Earthquake Emergency Foundation Data Spatialization and Regional Emergency Response Ability Estimation”, Institute of Geology, China Earthquake Administration (CEA) and Institute of Geographic Sciences and Natural Resource Research, Chinese Academy of Sciences (CAS) jointly developed earthquake emergency foundation dataset in km grid format in 2010.

In 2013, the dataset was updated with the census data of the year 2011. The dataset covers the Chinese mainland in its spatial range and has twenty thematic features, such as population, building and GDP. For this study, our aim was earthquake loss assessment, including the estimation of building damage and deaths; therefore, only the km grid format of the population data (Fig.1 A) and building data (Fig.1 B-E) were used in this study, as shown in Figure 1. The buildings were categorised into four types:

B1 type building (see Fig. 1 B): steel and steel reinforced concrete structure, i.e. high-rise steel structure, frame-shear wall structure, high-rise shear wall structure and multi-storey frame or high-rise frame structure. This type of building has the best anti-seismic capacity.

B2 type building (shown in Fig. 1 C): brick masonry structure; this type of structure is widely used in Chinese cities, its anti-seismic capacity is inferior to B1 type buildings.

B3 type building (shown in Fig. 1 D): brick house, open-space structure with 24 mm brick, cavity brick wall structure.

B4 type building (shown in Fig. 1 E): adobe houses mostly in Chinese rural villages. They have the worst anti-seismic capacity.

Figure. 1 Exposure data in km grid format. (A) Population data in km grid format; (B) B1 type building (steel and steel reinforced concrete structure) data in km grid format; (C) B2 type building (brick masonry structure) data in km grid format; (D) B3 type building (brick house, open-space structure with 24 mm brick, cavity brick wall structure) data in km grid format; (E) B4 type building (adobe houses mostly in Chinese rural villages) data in km grid format

3.2 Dasymetric model for the dataset generation

The data generation methods of this study are essentially a kind of regression method and are published in the Chen et al (2014); Han et al (2013); Jiang et al (2002). In order to make this

paper self-support, we take population data as an example to summarize the dasymetric data generation process, as described in the following steps.

Dividing regions for modelling: As the Chinese territory is large, the model for dasymetric data generation (disaggregating administration unit data to grid data) in different regions (i.e. province, city, county) should be defined separately. However, it would be too complicated to build a unique model for each region. As the source population census data used in the study are based on county level, so we select county as the basic modelling unit. We build fourty model regions from 2861 counties, according to their geographic and population characteristics such as population number, form and economy. In the modelled region, some typical counties (i.e. different average population density, different land use) have been sampled for regression analyses.

Selecting parameters for the model: Land use/land cover (LULC) data are widely used as auxiliary data (parameters) for the dasymetric data generation (Thieken et al, 2006; Jia et al, 2014). We also use a similar method to build the dasymetric model, in which the land use data are divided into sixty categories from the Landsat TM image. Then, the following six land use types are selected as the model parameters as they are considered to have high relativity with population distribution: the cultivated land, forest land, grass land, rural residential land, urban residential land, industrial and transportation land (Jiang et al, 2002).

Building the model: A linear regression method is used to build the model as shown in Eq. (1) and Eq. (2). The relationship between population density and different types of land use is built in Eq. (1).

$$P_j = \sum_{i=1}^{M} (p_{ij} \times s_{ij}) + B_j \qquad (1)$$

Where P_j is the total population in a county j, p_{ij} is average population density of the land use type i in the county j, s_{ij} is the area of the land use type i in the county j. M is the land use type count. p_{ij} and B_j are the regression parameters, which are solved by the method of least minimum square according to sample county data.

Then the population density in each grid can be calculated from Eq. (2),

$$G_k = \frac{\sum_{i=1}^{M} (p_{ik} \times s_{ik})}{\sum_{i=1}^{M} s_{ik}} \qquad (2)$$

where G_k is the population density in a km grid of the model region k, p_{ik} is the average population density of the land use type i in the grid, determined by Eq. (1), s_{ik} is the area of the land use type i in the grid; M is the land use type count.

4 Two-phase earthquake disaster estimation method supported by km grid format exposure data

Our estimation method consists two phases: a pre-earthquake phase and a co-earthquake phase. For the pre-earthquake phase, we pre-calculated earthquake loss according to earthquake description parameters and stored the pre-calculated loss estimation data in the database in km grid format. This means the earthquake loss was pre-estimated before it occurs according to appropriate scenario earthquake parameters. Having the exposure data in km grid format makes the disaster loss pre-calculation possible. Then, when the earthquake occurs, the disaster estimation becomes the extraction and statistics from the pre-calculated loss estimation data with regard to the range of its spatial influence. Generally, the studied method will go through two phases and then six stages, as shown in Table 1.

Table 1. Components and workflow of the two-phase earthquake disaster loss estimation method

4.1 Pre-earthquake phase

4.1.1 Determination of earthquake losses calculation factor

Earthquake movement for disaster loss estimation use many parameters, namely, surface wave magnitude (Ms), PGA, shaking map and spectral displacement (SD) (Eleftheriadou and Karabinis, 2011). Two factors were considered when we determine the calculation parameters of this study:

(1) Availability. As the primary objective of our investigation is to estimate earthquake disaster loss for the purposes of emergency response, the parameters sought for describing ground movement should be available in the co-earthquake period for the whole Chinese spatial range. As nationwide earthquake monitor network has been established by CEA. It can acquire four elements of data about the earthquake (epicentre location, time, magnitude, focal depth) within several minutes after an earthquake for the whole Chinese territory. Publishing these four earthquake elements is the official job of CEA. Since the data on the four earthquake

elements are released by a government department (CEA), this guarantees their authoritativeness and availability at any time for comparison with other ground movement parameters. So, we primarily considered selecting them as the earthquake disaster loss calculation factors.

(2) Accuracy. Although the disaster loss is highly related to the four earthquake elements (especially earthquake magnitude), these elements are too coarse to directly use for loss estimation. The damage caused by two earthquakes of the same magnitude, and even in same earthquake for the four elements can be quite different. For example, the earthquake elapsed time can have a great influence on earthquake damage, and even in one earthquake the damage at different spatial locations is also different. So, in earthquake engineering, seismic intensity is often used to mark the exposure damage. We finally selected this parameter as the disaster calculation factor for earthquake emergency disaster loss assessment. In a real earthquake, the seismic intensity field of influence can be inferred from the four earthquake elements through the earthquake grade-intensity attenuation relationship. We will introduce this in the next section.

4.1.2 Gridding DPM

Building a vulnerability assessment is the foundation for population loss estimation. According to the *Technical Rules for Earthquake Disaster Prediction and Related Information Management* (GB/T19428-2003, 2003), building damage is classified into five categories in China: no damage, slight damage, moderate damage, serious damage and collapse. As shown in Figure 1, the building exposure data are classified into four categories according to their structure and anti-seismic characteristics.

In the CEA, the most widely used building vulnerability assessment method is Eq. (3) (Yin, 1995), which is essentially a kind of DPM model:

$$D_{Sj}(I) = P\left[D_j \middle| I\right] B_S, \quad (3)$$

where I is seismic intensity, S is the building type, $P\left[D_j|I\right]$ is damage ratio of S type building under I intensity, which is a kind of DPM, and B_S is the total building area of S type building.

The DPM (referring to $P\left[D_j|I\right]$) is the key of the estimation. The DPM for this study come from Yin (1995) and is deduced from the hybrid method, which spatially includes the whole

Chinese mainland area. In Table 2 we present part of the DPM for the B1-type building as an example to explain its meaning. The earthquake disaster risks of different regions are different, which is represented in the earthquake intensity zoning map of China released by the CEA, shown in Figure 2. This map depicts the possible maximal seismic intensities that the different regions of China may face in future (seismic intensity with exceedance probability of 10% in the next 50 years), which represents the actual earthquake disaster hazard. When people construct a building in the region with a high possible intensity value, they need to ensure the building has high anti-seismic capacity, which is compulsory according to the Chinese laws. This also means the same type of building in different possible earthquake intensity zones can have different anti-seismic abilities. Thus, the DPM values in different possible seismic intensity regions are different in Table 2.

Figure 2. Earthquake intensity zoning map of China (3rd generation).

Generally, seismic intensity represents the damage power and the related destruction caused when the earthquake strikes. According to *China Seismic Intensity Scale* (GB/T 17742-1999, 1999), seismic intensity in China ranges from I to XII. When the seismic intensity at a place caused by an earthquake is less than VI, no damage can be considered to have occurred, and at the upper end of the range, no earthquake of a seismic intensity of XII has been recorded in China. So in this study, the column values of the DPM range from VI to X, as shown in Table 2. Thus, the table values indicates the damage ratio, for example, when a high-rise building with a shear wall structure (B1 type) is struck by an earthquake of seismic intensity VIII and if it is located in possible seismic intensity zone VI, the damage ratio for “no damage” is 40%, but if it is located in possible seismic intensity zone VII, the ratio is 55%.

Table 2. DPM of A type building in possible VI and VII region (%) (adapted from Yin, 1995)

The exposure data is in km grid format, as in Figure 1, so we grid the DPM for the convenience of the loss calculation with the support of GIS.

The gridding of the DPM has two steps: (1) The DPM tables have been associated with the vector map of the earthquake zoning of China, by “regional intensity”, as shown in Figure 2. (2) The vector map has been then converted to a grid map where the cell values depend on the DPM tables. The grid map have the same cell size with the exposure maps.

4.1.3 Building vulnerability assessment data generated in km grid format

After the gridding operation, the DPM is in a km grid format. Then, Eq. (3) is realized by the map algebra shown in Figure 3, which is also in km grid format. As a result of the spatial multiplication operation, a total of 100 layers are obtained including four types of buildings, with five damage degrees (from "no damage" to "collapse") and five seismic intensity levels (from VI to IX).

Figure 3. Building vulnerability data calculation process based on map algebra.

4.1.4 People loss data generation in km grid format

Many factors are related to deaths in an earthquake, including the building damage, population density, and earthquake occurrence time and rescue countermeasures. Among them, building damage is the key factor (GB/T19428-2003, 2003).

A regression model is used in this study, as in Eq. (4) (Ma and Xie, 2000):

$$log(RD) = 9.0(RB)^{0.1} - 10.07; \quad ND = f_t f_p (RD)P \qquad (4)$$

where ND is the number of deaths, RD is people death ratio, RB is the building collapse ratio, P is the total number of people in the calculation area, f_t is the fixed time factor, and f_p is the people density fix factor. f_p is determined by Table 3 (Ma and Xie, 2000).

Table 3. Value of f_p

The ratio of people in a building has a great influence on loss of life in an earthquake, which is affected by the time of a day. Time factor f_t is 1 in the daytime, and a different value is given regarding the different seismic intensities at night, as shown in Table 4 (Ma and Xie, 2000).

Table 4. Value of f_t in night-time

Using map algebra method, people loss estimation data are generated in km grid format, which consists of two time periods (daytime and night-time) and five intensity ranges (from VI to XI), making a total of 10 layers.

Using this method, we developed a pre-calculated earthquake loss estimation data set in km grid format, using the Python 2.7 and ArcGIS Desktop 10.1 program. The ArcGIS file geodatabase was used to store and manage the loss data, including 100 building damage layers and ten people loss layers. Some of them are shown in Figure 4.

Figure 4. Pre-calculated earthquake loss estimation dataset (selected). (A) "Collapse" under intensity X of B1 type building; (B) people loss under intensity X in daytime.

4.2 Co-earthquake phase

4.2.1 Generating theoretical isoseismal map

The isoseismal map is used to show lines of equal felt seismic intensity, which depict the seismic field of influence of the earthquake. The loss estimation is for emergency response; we used a theoretical isoseismal map as a substitute for the real isoseismal map, which is produced from field investigations several days to several month after an earthquake.

The theoretical isoseismal map is generated in the following two steps:

(1) Locating the earthquake position and determining the rupture direction of the fault zone causing the earthquake. For this, a Chinese nationwide fault zone distribution map is stored in the ArcGIS geodatabase in which the fault zone direction is recorded. Thus, after an earthquake we can quickly locate the earthquake position on this map and use the nearest fault zone direction as the fault rupture direction of the earthquake.

(2) Then, the earthquake magnitude-intensity attenuation relationship is used to generate isoseismal lines from seismic intensity VI to its maximum theoretical intensity. Spatially, the theoretical earthquake intensity is an ellipse. Eqs. (5) and (6) are the most widely used for establishing the attenuation relationship, fitting east China and west China separately. The east longitude 107.5^{o} is considered as the dividing line between east China and west China (CEA, 2010). If the longitude of the epicentre is greater than 107.5^{o}, then Eq. (5) will be used. Otherwise Eq. (6) is used.

$$I_\alpha = 6.046 + 1.480M_s - 2.081\ln(R_\alpha + 25) \quad I_\beta = 2.617 + 1.435M_s - 1.441\ln(R_\beta + 7) \quad (5)$$

$$I_\alpha = 5.643 + 1.538M_s - 2.109\ln(R_\alpha + 25) \quad I_\beta = 2.941 + 1.303M_s - 1.494\ln(R_\beta + 7) \quad (6)$$

where I_α, I_β are the average intensity around the ellipse long axis and short axis; R_α、R_β are the short and long axis of the ellipse, the unit is km； and M_s is the earthquake grade.

The Eqs. (5) and (6) is transformed to Eqs. (7) and (8). Once Ms and I_α (I_α always equates to I_β) are determined, the length of the short axis (R_α) and long axis (R_β) of the ellipse can be

calculated. I_α ranges from 6 to max intensity. Because the lengths of R_α and R_β should be greater than zero, which controls the range of $I_\alpha(I_\beta)$ from six to maximum intensity.

$$R_\alpha = e^{(6.046+1.480M_s - I_\alpha)/2.081} - 25 \qquad R_\beta = e^{(2.617+1.435M_s - I_\beta)/1.441} - 7 \qquad (7)$$

$$R_\alpha = e^{(5.643+1.538M_s - I_\alpha)/2.109} - 25 \qquad R_\beta = e^{(2.941+1.303M_s - I_\beta)/1.494} - 7 \qquad (8)$$

Then the theoretical isoseismal map of the earthquake can be quickly generated. The isoseismal map for Minxian earthquake is shown in Figure 5 as an example.

Figure 5. Theoretic isoseismal map of the Minxian earthquake.

4.2.2 Extraction of statistics on disaster loss

In this stage, the disaster loss calculation essentially becomes a spatial extraction of statistics of pre-calculated disaster loss estimation data, according to the spatial distribution of the theoretical isoseismal map. The steps are as follows:

(1) First, we separately build isoseismal polygons according the seismic intensity value. These isoseismal polygons are then converted into raster (km grid) format, with the intensity value being their attribute value.

(2) Then, the loss data associated with different seismic intensities are retrieved from the pre-calculated loss estimation dataset. The isoseismal polygon with a certain intensity (for example intensity VI) is used as spatial query condition to extract the disaster data within the polygon from the retrieved data. We repeat the query and extraction to the maximum seismic intensity.

(3) The people losses from each queried result are counted.

(4) The losses are summed to obtain the final loss for the earthquake.

5 Validation and discussion

5.1 Validation

In order to validate and test the effectiveness of the pre-calculation loss estimation data and corresponding loss estimation method, we selected four actual destructive earthquakes

occurring on the Chinese mainland as the experimental cases, which are shown in Figure 6; the four elements used for the damage loss estimation are displayed in Table 5.

Figure 6. The locations of the four real earthquakes used as experimental cases.

Table 5. Basic information on experimental cases

Figure 1 shows the exposure data (building and population) as a dasymetric map in km grid format. In order to compare with the administrative unit-based exposure data support loss estimation method, we used the city as the statistics unit and summed up the grid values of the dasymetric map within a city range to generate the administration unit-based exposure data.

The traditional earthquake loss estimation method was used for the test, which includes the following steps: (1) according to the four earthquake elements, a theoretical isoseismal map is generated; (2) according to the spatial distribution of seismic intensity in the isoseismal map, the building damage is separately calculated by the DPM; and (3) the people losses are calculated based on building damage. In this estimation process, the disaster losses are not pre-calculated before the earthquake, and all disaster losses are calculated on the fly.

In the case studies, the building damage estimation and people loss estimation are based on identical calculation formulae, as shown in Eq. (3) to Eq. (6). We used an identical hardware environment for the two estimations, which was used to realize the calculation process: Intel Core2 Quad CPU Q9550 @ 2.83GHz, 4.00GB RAM, Windows 7 Pro 32-Bit with SP1 in PC. Python 2.7 and ArcGIS Desktop 10.1.

We selected people losses as the estimation aim. There are three reasons for this selection: human losses are more important than building damage losses for earthquake emergency response; human loss estimation appears to be more sophisticated and time-consuming since it is based on building damage loss estimation; and, real people loss value in the actual earthquakes are easy to collect and are confirmed by the government at all levels. Thus real human loss values are more authentic and accurate than the building losses in these real earthquakes.

In these case studies, we mainly focused on the evaluation speed and accuracy, but especially speed (for earthquake emergency response and rescue, speed is more important than accuracy), and the results are shown in Table 6.

Table 6. Comparison of calculation speed and accuracy for experimental cases

5.2 Discussion

The experiment shows that the earthquake disaster loss estimation method explored in this study can significantly improve the estimation speed. The disaster estimation can be done within a single minute on a normal personal computer, even when facing a huge earthquake like the Wenchuan earthquake (Ms 8.0). The reason for this quick speed is the pre-calculation of the disaster loss before the earthquake's occurrence. So after the earthquake, the disaster estimation literally becomes the disaster loss spatial statistics according to the seismic intensity field. The pre-calculated disaster loss method benefits from the dasymetric map approach. Without the support of the km grid format exposure data, it would be hard to perform a meaningful pre-calculated disaster loss estimation. The other benefit of this pre-calculation method is that we can directly estimate the loss of lives. However, in the traditional method, it is necessary to go through the building damage estimation on the fly before the people loss estimation.

However, this earthquake disaster estimation method also greatly depends on dasymetric exposure data, which increases the difficulty in the production of the exposure data. Although the dasymetric population data development method and product are increasingly popular and easy to available, it is still not easy to obtain appropriate data in many countries and regions, especially in some undeveloped regions. Meanwhile, the building of areal exposure data and corresponding methods are lacking even in developed countries and regions (Han et al., 2013). In this study, we pre-calculated the earthquake losses to improve the estimation speed, but flexibility was also lost in the disaster loss estimation. The updating of the disaster exposure data, calculation parameters or calculation formulae will cause the whole pre-calculated disaster loss estimation data to be revised. Furthermore, the pre-calculation disaster loss estimation data will consume some hardware storage: in our study 5.98 GB was used for the storage of these pre-calculated disaster loss estimation data (building damage and population loss in ArcGIS file geodatabase format). With the development of computer hardware, it does not seem a big issue considering the improvement in estimation speed.

As shown from the experiment results, the accuracy of disaster loss estimation of the studied method is also improved. The reason is the spatial disparity considered in the dasymetric exposure data. Taking population distribution as an example, if just part of an administration unit has been affected by an earthquake disaster, how many population in this unit should be used for loss estimation calculation? The administration unit supported method assumes the

exposure data averagely distributed inside the census units, as shown in Figure 7-A, and Eq. (9) is used for determining the population number in disaster loss calculation.

$$Pop_{inf} = \left(\frac{Area_{inf}}{Area_{county}}\right) * Pop_{county} \qquad (9)$$

Where Pop_{inf} is the influenced population by the disaster, $Area_{inf}$ is the influenced area in the county (the area of the yellow polygon in the Figure 7-A), $Area_{county}$ is the area of the county, Pop_{county} is the population of the county.

However, this assumption is inappropriate because population is not spatially evenly distributed in the whole administration unit. Generally people tends to live around the main settlement points such as the village or city centre. Figure 7-B shows the real population distribution, in which case only a very small proportion of the population are located in the disaster influence area. So Eq. (9) will produce a large error in people loss estimation. While dasymetric exposure population data provide good description on such case as shown in the Figure 7-C. The population data used for disaster loss calculation is based on the sum of all the influenced population grids. Therefore, it is easy to improve estimation accuracy of an earthquake whose exposure data in the influenced area have high spatial disparity.

Figure 7. The representation of spatial distribution of population exposure data. The points represent population distribution. The area surrounded by red lines represents the affected disaster area in an administration unit. (A) Average distribution inside the whole administration unit; (B) Actual distribution according to settlements. (C) Gridded distribution supported by dasymetric map approach.

The experiment reveals that the estimation result for the Ludian earthquake has large deviations from actual losses. The reason is that the human loss estimation considers building damage as the only contributing factor. However, people live in the mountainous areas as 87% of Ludian County is mountainous. After the earthquakes, serious secondary geological hazards occurred. Field investigation after Ludian earthquake shows that about one third of people loss were caused by secondary geological hazards (China Earthquake Administration, 2015). In Minxian earthquake there is a similar situation, as parts of villages were even covered by debris flow.

The deviations found in all of the four cases are led by several reasons. Identical theoretical isoseismal map has been used both in the traditional estimation method and in the two-phase

method. We believe the inconsistency between theoretical isoseismal map and actual isoseismal map is one of reasons that cause the deviations. Because actual isoseismal map of an earthquake is usually plotted several days to several months after the earthquake field investigation, we use the theoretical isoseismal map to substitute the actual one in disaster estimation for emergency response. Theoretical isoseismal map is established from the Eqs. (7), (8), which is deduced from regression analysis of historical isoseismal maps. Although the inconsistency is well known in Chinese earthquake engineering field, the theoretic isoseismal map is still widely used for co-earthquake disaster estimation for two reasons: (1) there is no better alternative; (2) the deviation caused by this inconsistency is limited (China Earthquake Administration, 2015). Shakemap has good potential in solving this problem, but currently it is still under development in China.

Meanwhile, the km grid exposure data has great influence on the two-phase disaster estimation method. The accuracy of the km grid exposure data should be emphasized, when we use the two-phase method. Some dasymetric map approaches or exposure data are recommended, such as the regression method supported by land use/land cover (LULC) data, LandScan dataset (http://web.ornl.gov/sci/landscan/).

The pre-calculated km grid-based disaster loss estimation data not only improve the disaster estimation speed and accuracy, but also generate extra value in earthquake emergency response. We take the Wenchuan earthquake as an example, the earthquake disaster loss estimation result represents not just number of deaths like the traditional method. It also provides the spatial distribution of the possible loss of lives, as shown in Figure 8. This provides useful guidance to disaster area emergency rescue actions and for the emergency evacuation of people. Meanwhile, this study provides an applied example of improving earthquake disaster analysis using exposure data in areal format. It has good potential for application in risk analysis and loss estimation for other kinds of disasters.

Figure 8. Spatial distribution of prediction of possible deaths in the Wenchuan earthquake.

6 Conclusion

The rapid and accurate estimation of earthquake disaster losses in the period up to 2 hours after an earthquake is crucial for earthquake emergency response and rescue (Nie et al., 2012). It is also the key motivation for this study. A new earthquake disaster loss estimation method

for earthquake emergency response based on dasymetric exposure data was successfully performed. The method consists of two phases: a pre-earthquake phase and a co-earthquake phase. In the pre-earthquake phase, in four stages, disaster losses have been pre-calculated and stored as a dasymetric map in km grid format, thereby benefiting from the areal format of exposure data. Then, in the co-earthquake phase, the calculation of disaster loss is based on the spatial statistics of the pre-calculated disaster loss estimation data according to the seismic intensity influence field. The core contributions of this study are the development of earthquake disaster loss estimation areal data and a corresponding new two-phase earthquake disaster loss estimation method, which makes it possible to estimate the disaster losses of random earthquakes before or at the point of their occurrence. This not only improves the speed and accuracy of earthquake disaster estimation for co-earthquake response, but also serves as an earthquake disaster risk analysis before the earthquake occurrence.

Four recent real earthquakes that have occurred on the Chinese mainland were selected as the experimental cases to validate the new method. The estimation of deaths is separately tested. We conclude that the studied estimation method is effective in improving the speed and accuracy of earthquake loss estimation. The estimation time can be reduced to a significantly shorter time, even when faced with a huge earthquake like Wenchuan earthquake using a normal personal computer. Although, improvements have been found in the accuracy of the studied estimation method, deviation between estimated losses and real losses in the Ludian and Minxian earthquakes are also found, which cannot be overlooked. This indicates that serious consideration should be given to how the secondary geological disaster impact of earthquakes influences people death estimation, especially for the mountainous areas, which are widespread in south-west China. It is also the most frequent area of earthquake occurrences in China.

The pre-calculated disaster loss estimation data in km grid format also enriches the disaster loss estimation by providing a spatial distribution of possible deaths and building damage. This will be of benefit to earthquake response rescue services and rescue evacuation.

Currently, the pre-calculated earthquake loss estimation areal data and corresponding two-phase loss estimation method are used by the CEA. In future, we will explore the influence of the secondary geological disaster on the estimation of human losses in mountainous areas. The automatic generation of earthquake response countermeasures using

earthquake emergency response knowledge (Xu et al., 2014) from estimated earthquake disaster losses is another study direction that we will pursue in the future.

Acknowledgments

This work was supported in part by grants from the National Key Technology R&D Programme of China (Grant No. 2012BAK15B06), the Special Fund for Basic Scientific Research Operations of the Institute of Geology, CEA (Grant No. IGCEA1109), the National Natural Science Foundation of China (Grant No.40901272), Open Research Fund Program of Shenzhen Key Laboratory of Spatial Smart Sensing and Services (Shenzhen University) (Grant No. 201404) and Jiangsu Surveying, Mapping and Geoinformation Science Research Project (Grant No. JSCHKY201506).

The authors would like to express their appreciation to Dr. Scott Miles at Western Washington University, Dr. Wenxia Tang at Central China Normal University for their valuable helps. The authors also wish to thank the editor and the two referees for their comments and suggestions that greatly improved this manuscript.

References

Alahmadi, M., Atkinson, P., and Martin, D.: Estimating the spatial distribution of the population of Riyadh, Saudi Arabia using remotely sensed built land cover and height data, Comput. Environ. Urban, 41, 167–176, 2013.

Alam, M. N., Tesfamariam, S., and Alam, M. S.: GIS-based seismic damage estimation: case study for the City of Kelowna, BC, Nat. Hazards Review, 14, 66–78, 2013.

Anagnos, T., Rojahn, C., and Kiremidjian, A. S.: NCEER-ATC joint study on fragility of buildings, Techn. Rep. NCEER 95-0003, State Univ. of NY at Buffalo, 1995.

Armenakis, C: Estimating spatial disaster risk in urban environments, Geomatics Natural Hazards & Risk, 4, 289–298, 2013.

ATC, Earthquake damage evaluation data for California, ATC-13 Report, Applied Technology Council, Redwood City, California, 1985.

Balk, D. and Yetman, G.: The global distribution of population: evaluating the gains in resolution refinement, Center for International Earth Science Information Network (CIESIN), Columbia University, New York, 2004.

CIESIN, Center for International Earth Science Information Network: Global Rural Urban Mapping Project (GRUMP), Alpha Version: Urban extents, Center for International Earth Science Information Network (CIESIN), Columbia University, New York, 2004.

Chakraborty, J., Tobin, G. A., and Montz, B. E.: Population evacuation: assessing spatial variability in geophysical risk and social vulnerability to natural hazards, Nat. Hazards Review, 6, 23–33, 2005.

Chen, K. P., McAneney, J., Blong, R., Leigh, R., Hunter, L. and Magill, C.: Defining area at risk and its effect in catastrophe loss estimation: a dasymetric mapping approach, Appl. Geogr., 24, 97–117, 2004.

Chen, Z. T., Li, Z. Q., Ding, W.X. and Han, Z. H.:Study of Spatial Population Distribution in Earthquake Disaster Reduction—A Case Study of 2007 Ning'er Earthquake, Technology for Earthquake Disaster Prevention, 7: 273-284, 2012. (in Chinese)

China Earthquake Administration: Report on earthquake emergency disaster information recognition and evaluation technologies, Institute of Geology, China Earthquake Administration, Beijing, China, 1253 pp., 2010. (in Chinese)

China Earthquake Administration: Report on earthquake disaster information service and emergency response decision-making support platform, Institute of Geology, China Earthquake Administration, Beijing, China, 412 pp., 2015. (in Chinese)

Coburn, A. and Spence, R.: Earthquake Protection, 2nd edition, John Wiley and Sons, West Sussex, England, 2002.

Dmowska, A. and Stepinski, F. T.: High resolution dasymetric model of U.S demographics with application to spatial distribution of racial diversity, Appl. Geogr., 53, 417–426, 2014.

Dobson, J. E., Bright, E. A., Coleman, P. R., Durfee, R. C., and Worley, B. A.: LandScan: a global population database for estimating populations at risk, Photogrammetric Engineering and Remote Sensing, 66, 849–857, 2000.

Dymiotis, C, Kappos, A. J, and Chryssanthopoulos, M. C.: Seismic reliability of R/C frames with uncertain drift and member capacity. J Str. Engng. ASCE, 125, 9, 1038–1047, 1999.

Earthquake Emergency Rescue Department, China Earthquake Administrator: Earthquake Emergency Response, Seismological Press, Beijing, 2004. (in Chinese)

Eleftheriadou, A. K. and Karabinis A. I.: Development of damage probability matrices based on Greek earthquake damage data, Earthq. Eng. & Eng. Vib., 10, 129–141, 2011.

FEMA: HAZUSMH MR4 Technical manual, Washington, DC: Federal Emergency Management Agency, available from: https://www.fema.gov/media-library/assets/documents/24609?id=5120, 2003.

GB/T17742-1999: China seismic intensity scale, General Administration of Quality Supervision, Inspection, and Quarantine of P R China, 1999. (in Chinese)

GB/T19428-2003: Technology rule of earthquake disaster prediction and related information management, General Administration of Quality Supervision, Inspection, and Quarantine of P R China, 2003. (in Chinese)

Han, Z. H., Li Z. Q., Chen, Z. T., and Ding, W. X.: Population, housing statistics data spatialization research in the application of rapid earthquake loss assessment: a case of Yiliang earthquake, Seismology and Geology, 35, 894–906, 2013. (in Chinese)

Hassanzadeh R., Zorica N. B., Alavi R. A., Norouzzadeh M., and Hodhodkian H.: Interactive approach for GIS-based earthquake scenario development and resource estimation (Karmania hazard model), Computers & Geosciences, 51, 324–338, 2013.

Jia, P., Qiu, Y.L., and Gaughan, E. A.: A fine-scale spatial population distribution on the high-resolution gridded population surface and application in Alachua County, Florida, Applied Geography, 50, 99–107, 2014.

Jiang, D., Yang, X. H., Wang, N. B. and Liu, H. H.: Study on Spatial Distribution of Population based on Remote Sensing and GIS, Advance in Earth Sciences, 17, 734-738, 2002. (in Chinese)

Karimzadeh, S., Miyajima, M., Hassanzadeh, R., Amiraslanzadeh, R., and Kamel, B.: A GIS-based seismic hazard, building vulnerability and human loss assessment for the earthquake scenario in Tabriz, Soil Dyn. Earthq. Eng., 2014, 66, 263–280.

Kappos, A.J., Panagopoulos, G., Panagiotopoulos, C., and Penelis, G.: A hybrid method for the vulnerability assessment of R/C and URM buildings, Bull. Earthquake Eng., 4, 391–413, 2006.

Langford, M.: Rapid facilitation of dasymetric-based population interpolation by means of raster pixel maps, Comput. Environ. Urban, 31, 19–32, 2007.

Lin, J., Cromley, R., and Zhang, C.: Using geographically weighted regression to solve the areal interpolation problem, Annals of GIS, 17, 1–14, 2011.

Ma, Y. H. and Xie, L. L.: Methodologies for assessment of earthquake causality, Earthq. Eng. Eng. Vib., 20, 140–147, 2000. (in Chinese)

Martin, D.: Directions in population GIS. Geography Compass, 5, 655–665, 2011.

Mebarki, A., Boukri, M., Laribi, A., Farsi, M., Belazougui, M., and Kharchi, F.: Seismic vulnerability: theory and application to Algerian buildings, Journal of Seismology, 18, 2, 331–343, 2014.

Miao, C. G. and Nie, G. Z.: Exploration on mode of earthquake emergency command, Journal of natural disasters, 13, 48–54, 2004. (in Chinese)

Mocormack, C. and Rad, F. N.: Earthquake loss estimation methodology for buildings based on ATC-13 and ATC-21, Earthquake Spectra, 1, 605–621, 1997.

Nadim, F., Moghtederi-zadeh, M., Lindholm, C., Anderson, A., Remseth, S., Bolourchi, M., Mokhtari, M., and Tvedt, E.: The Bam earthquake of 26 December 2003, B. Earthq. Eng., 2, 119–153, 2004.

National Research Council (NRC): The Impacts of Natural Disasters: A Framework for Loss Estimation, National Academy Press, Washington DC, 1999.

Nie, G. Z., An, J. W., and Deng, Y.: Advances in earthquake emergency disaster service, Seismology and Geology, 34, 782–791, 2012. (in Chinese)

Nie, G. Z., Chen, J. Y., Li, Z. Q, Su, G. W., Gao, J. G., and Liu, H. M.: The construction of basic database for earthquake emergency response, Earthquake, 22,105–112, 2002. (in Chinese)

Panahi, M., Rezaie, F., and Meshkani, S. A.: Seismic vulnerability assessment of school buildings in Tehran city based on AHP and GIS, Nat. Hazard. Earth Sys., 14, 4, 969–979, 2014.

Thieken A. H., Muller M., Kleist L., Seifert I., Borst D., and Werner U.: Regionalisation of asset values for risk analyses, Nat. Hazard. Earth Sys. Sci., 6, 167–178, 2006.

Whitman R. V., Reed, J.W., and Hong, S. T.: Earthquake damage probability matrices, www.iitk.ac.in/nicee/wcee/article/5_vol2_2531.pdf, 1973.

Xu, J. H., Nie, G. Z., and Xu, X.: A digital social network for rapid collection of earthquake disaster information, Nat. Hazard. Earth Sys., 13, 385–394, 2013.

Xu, J. H., Nyerges, L. T. and Nie, G. Z: Modeling and representation for earthquake emergency response knowledge: perspective for working with geo-ontology, INT. J. GEOGR. INF. SCI., 28, 185-205, 2014.

Yin, Z. Q.: Earthquake Disaster and Loss Prediction Method, Seismological Press, Beijing, 1995. (in Chinese)

Table 1. Components and workflow of the two-phase earthquake disaster loss estimation method

Phase	Stages
Pre-earthquake	Determining earthquake loss calculation factor
	Gridding damage probability matrices
	Building damage calculation
	People loss calculation
Co-earthquake	Generating theoretical isoseismal map
	Extraction of statistics on disaster loss

Table 2. DPM of A type building in a possible VI and VII region (%) (adapted from Yin, 1995)

Table 2-a. The DPM in a possible VI region

I	N	Sl	M	Se	C
Ⅵ	85	15	0	0	0
Ⅶ	60	35	5	0	0
Ⅷ	40	36	21	2.5	0.5
Ⅸ	20	0.37	28	12.5	2.5
Ⅹ	10	15.5	39.5	25.5	9.5

Table 2-b. The DPM in a possible VII region

I	N	Sl	M	Se	C
Ⅵ	88	12	0	0	0
Ⅶ	75	23	2	0	0
Ⅷ	55	33	10.3	1.5	0.2
Ⅸ	35	30.5	25.5	7.5	1.5
Ⅹ	15	20.5	40.5	16.5	7.5

Note: I = seismic intensity; N = no damage; Sl = slight damage; M = moderate damage; Se = serious damage; C = collapse. We omit the DPM for VIII and IX regions, since they are similar.

Table 3. Value of f_p

Population density	<50/km^2	50–200 /km^2	200–500 /km^2	>500 /km^2
f_p	0.8	1.0	1.1	1.2

Table 4. Value of f_t in the night-time

Intensity	Ⅵ	Ⅶ	Ⅷ	Ⅸ	Ⅹ

f_t	17	8	4	2	1.5

Table 5. Basic information on experimental cases

Case ID	Earthquake name/location	Earthquake time	Magnitude (Ms)	Focal Depth (km)
E1	Wenchuan, in Sichuan （31.0°N，103.4°E）	2008-05-12 14:28	8.0	14
E2	Yiliang, in Yunnan, （27.6°N，104.0°E）	2012-09-07 11:19	5.7	14
E3	Minxian, in Gansu （34.5°N，104.2°E）	2013-07-22 07:45	6.6	20
E4	Ludian, in Yunnan （27.1°N，103.3°E）	2014-08-03 16:30	6.5	12

Table 6. Comparison of calculation of speed and accuracy for experimental cases

Performance	Estimation method	E1	E2	E3	E4
Time consumed	No grid data support (traditional method)	27 minutes	7.8 minutes	8.7 minutes	8.5 minutes
	Grid data support (two-phase method)	38 seconds	26 seconds	30 seconds	29 seconds
People loss estimation accuracy	No grid data support (traditional method)	170,739 (246.7%)	31 (38.8%)	68 (71.6%)	237 (38.4%)
	Grid data support (two phase method)	63,093 (91.1%)	75 (93.8%)	70 (73.7%)	369 (59.8%)
Real people loss		69,227	80	95	617

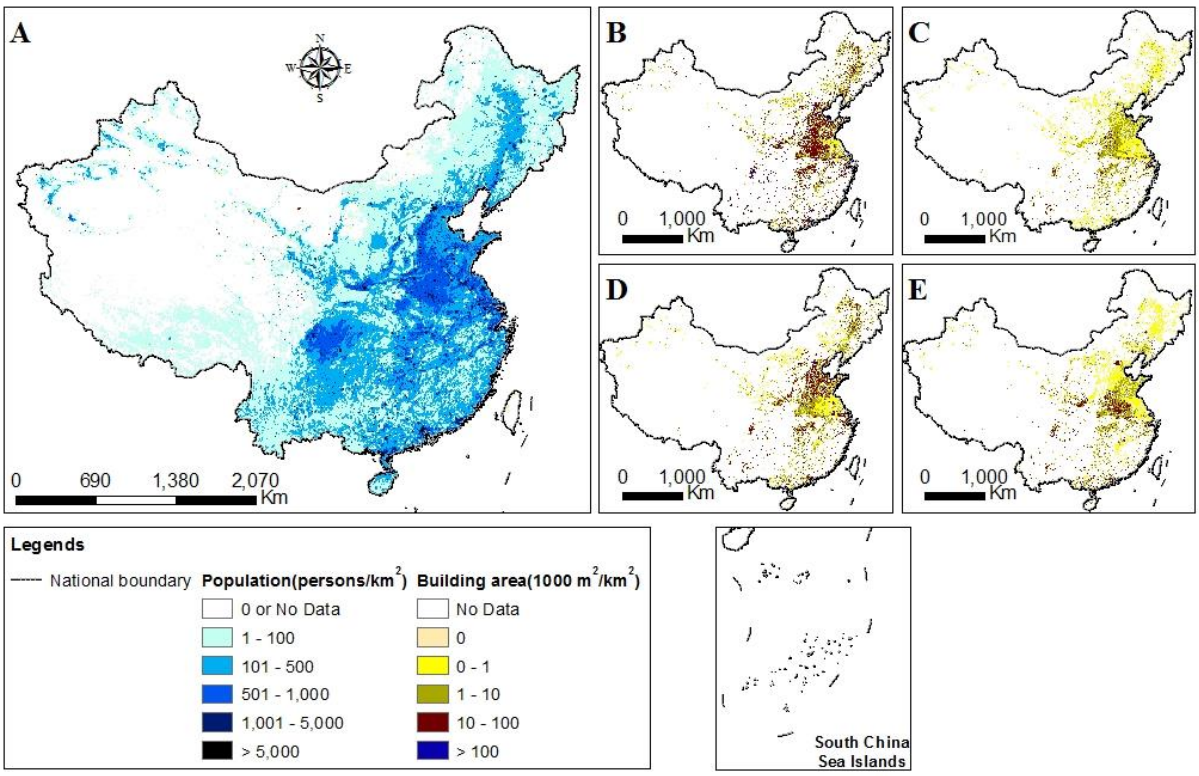

Figure 1. Exposure data in km grid format. (A) Population data in km grid format; (B) B1 type building (steel and steel reinforced concrete structure) data in km grid format; (C) B2 type building (brick masonry structure) data in km grid format; (D) B3 type building (brick house, open-space structure with 24 mm brick, cavity brick wall structure) data in km grid format; (E) B4 type building (adobe houses mostly in Chinese rural villages) data in km grid format

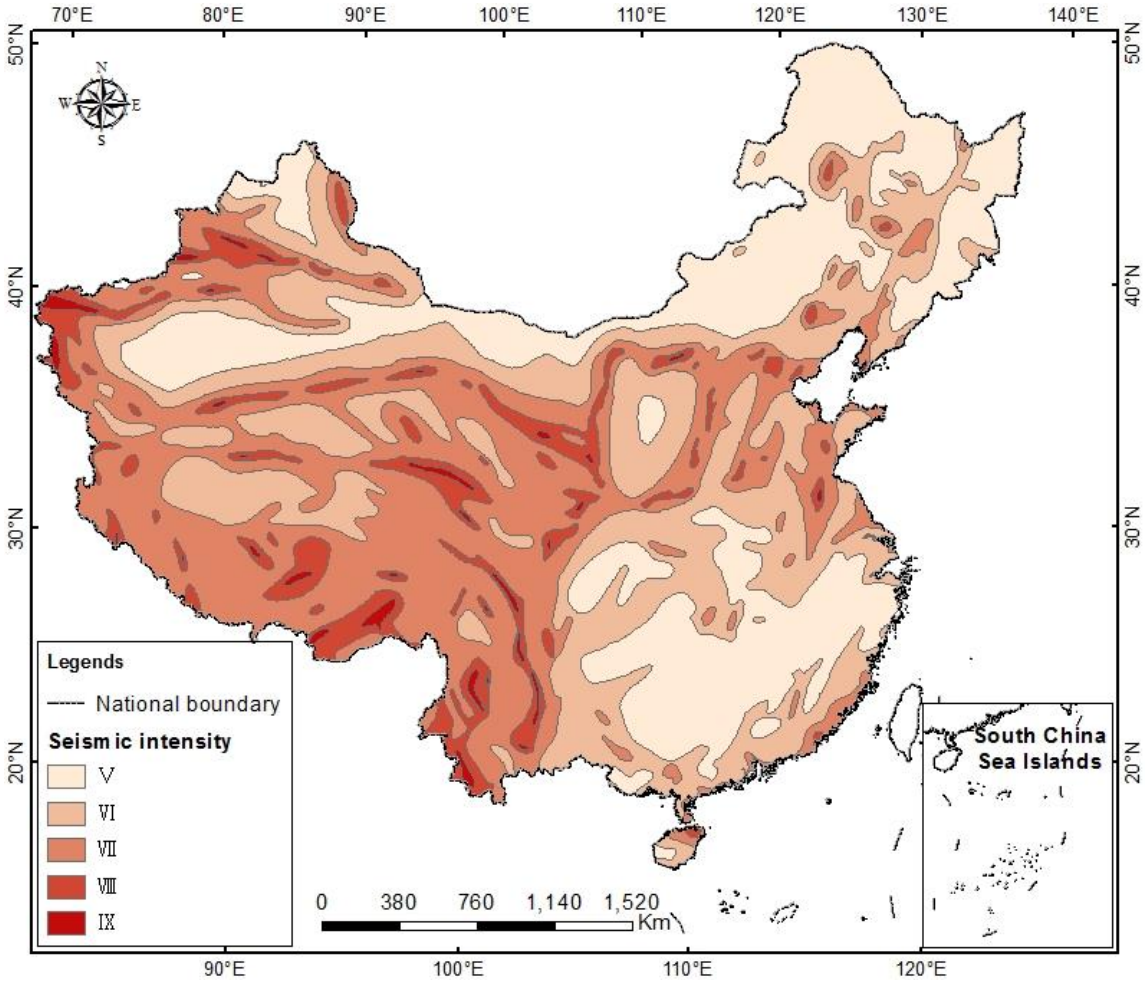

Figure 2. Earthquake intensity zoning map of China (3rd generation).

Regional Intensity	Building Type	DMP Value 1	DMP Value 2	.....
6	B1	0.85	0.15	.....
7	B1	0.65	0.35	.....
.....	.....	.....	.....	.....

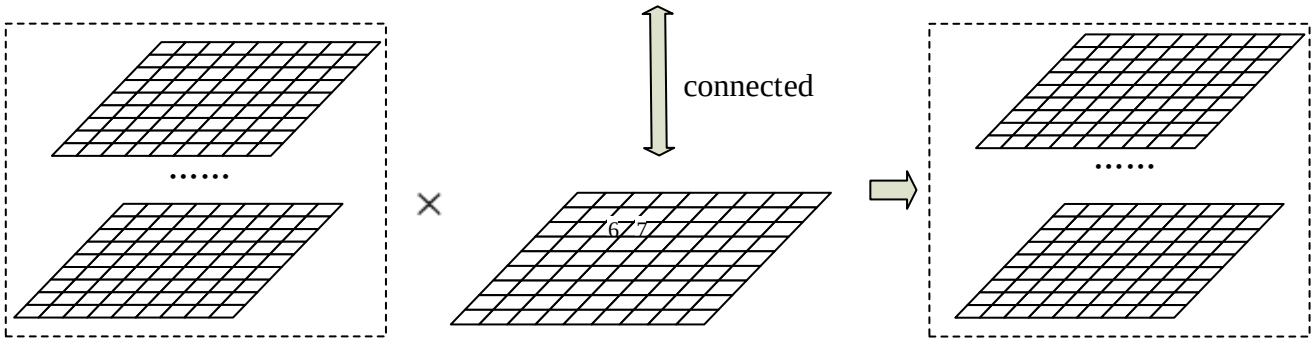

1

2

3 Figure 3. Building vulnerability data calculation process based on map algebra.

4

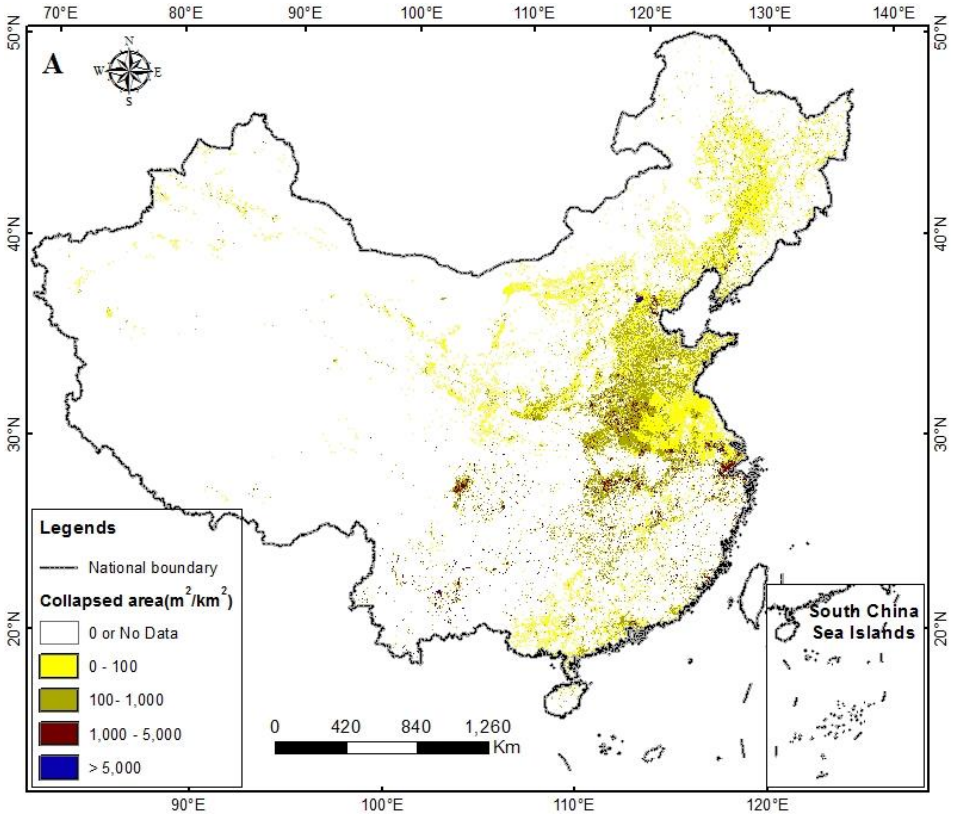

1

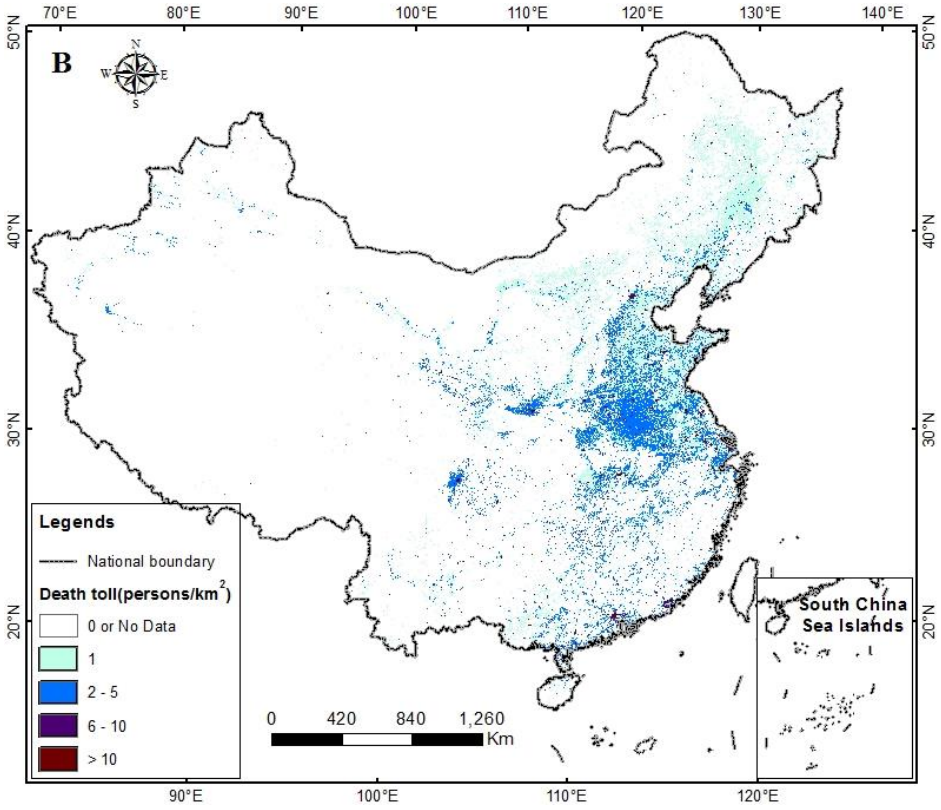

2

3 Figure 4. Pre-calculated earthquake loss estimation data set (selected). (A) "Collapse" under
4 intensity X of B1 type building; (B) people loss under intensity X in daytime.

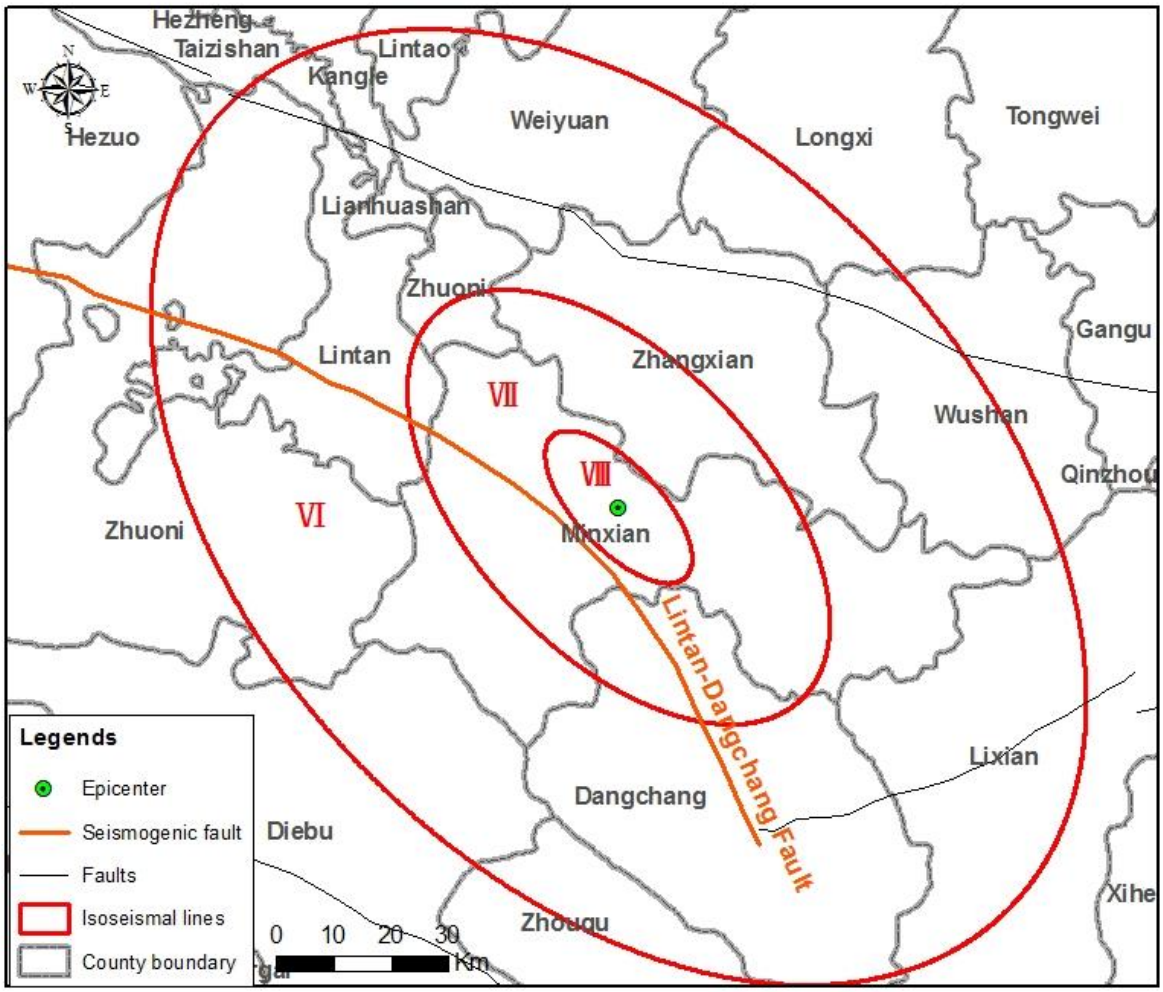

Figure 5. Theoretic isoseismal map of the Minxian earthquake.

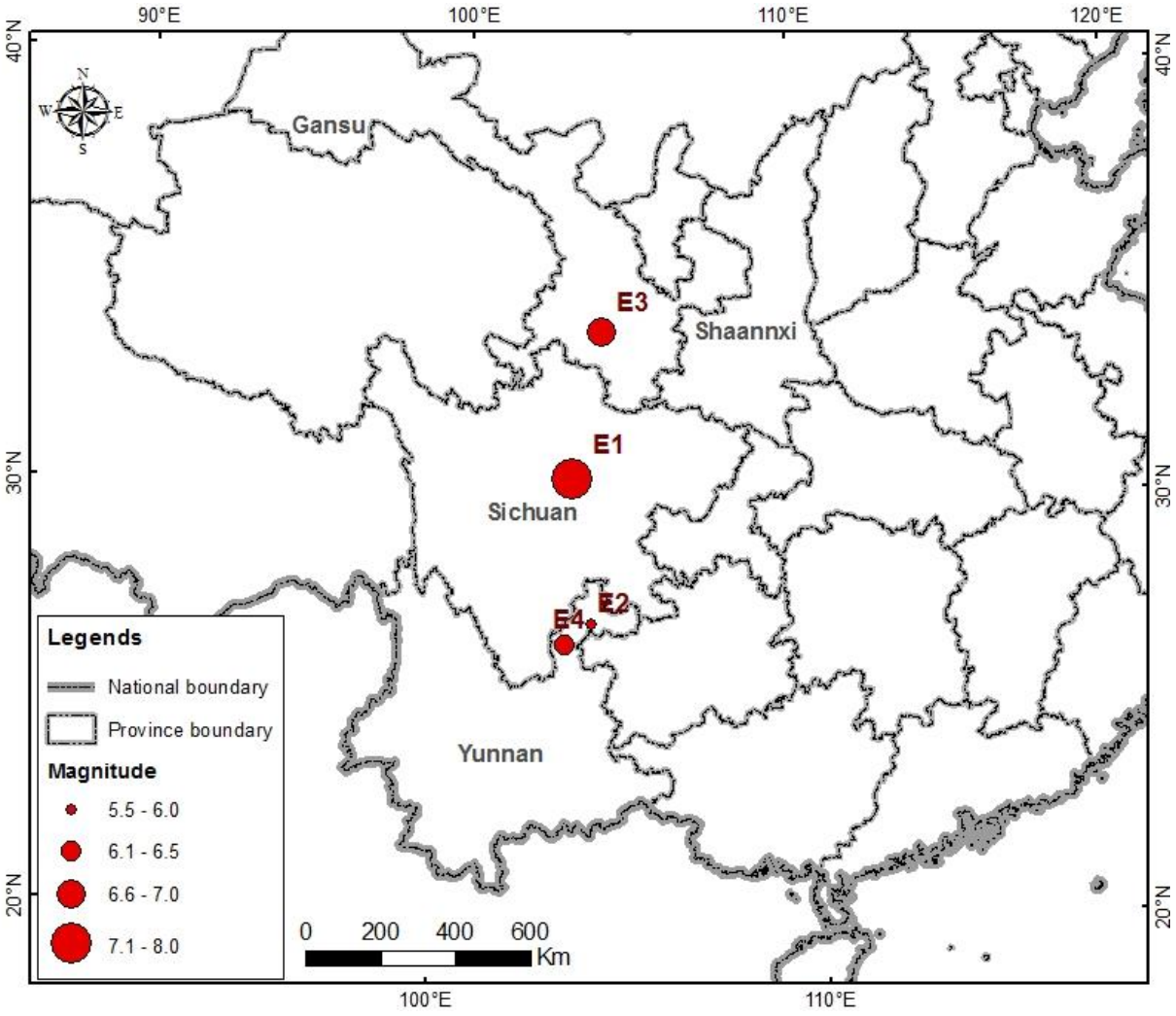

Figure 6. The locations of the four real earthquakes used as experimental cases.

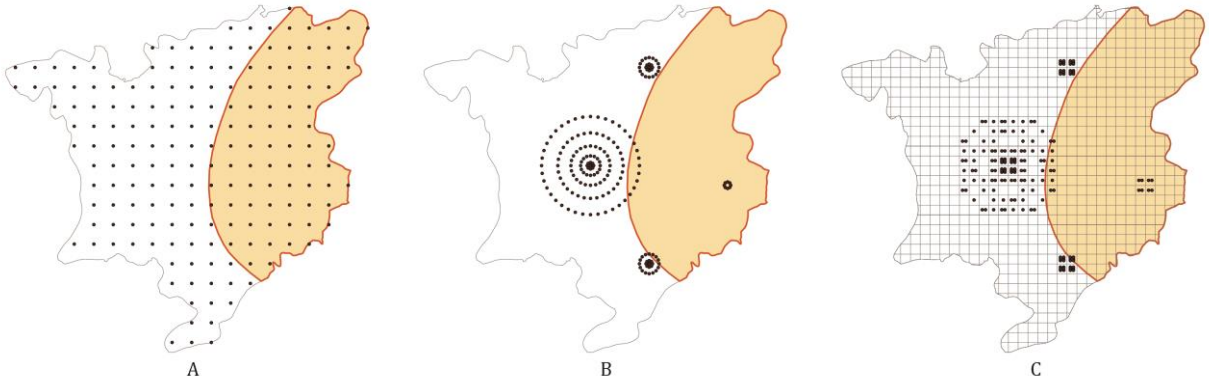

Figure 7. The representation of spatial distribution of population exposure data. The points represent population distribution. The area surrounded by red lines represents the affected

disaster area in an administration unit. (A) Average distribution inside the whole administration unit; (B) Actual distribution according to settlements. (C) Gridded distribution supported by dasymetric map approach.

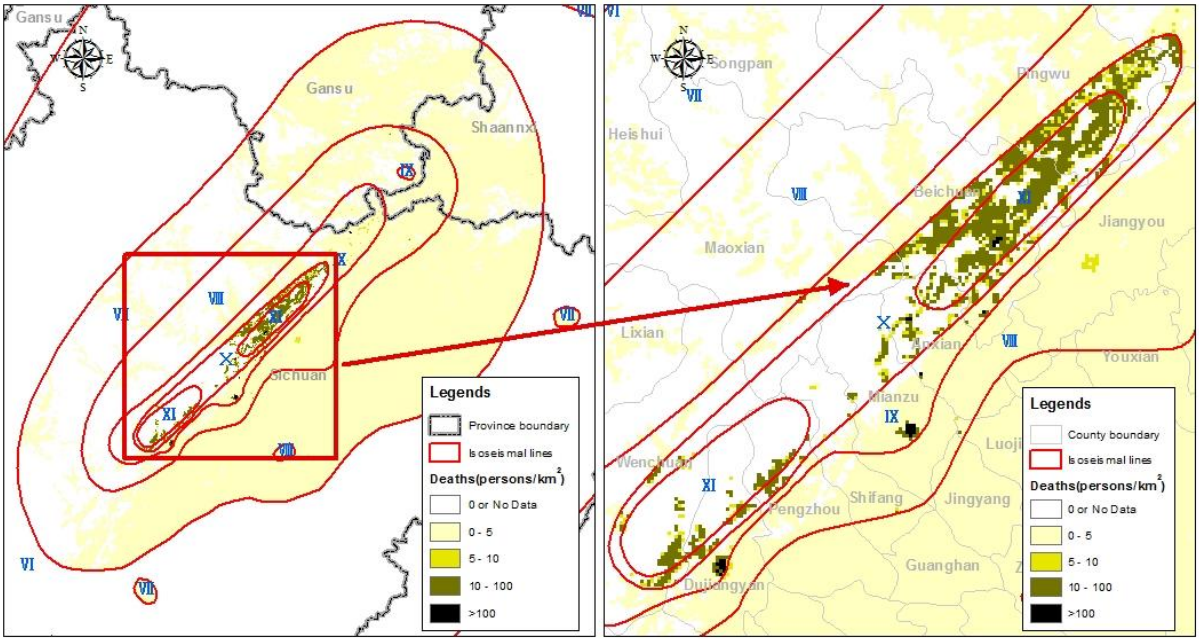

Figure 8. Spatial distribution prediction of possible deaths in the Wenchuan earthquake.